USGS
science for a changing world

U.S. DEPARTMENT OF THE INTERIOR
U.S. GEOLOGICAL SURVEY

PRELIMINARY SCIENTIFIC RESULTS OF THE CREEDE CALDERA CONTINENTAL SCIENTIFIC DRILLING PROGRAM

P.M. Bethke, Editor

Open-File Report 94-260-N

2001

TRANSPORT IN POROUS AND FRACTURED MEDIA OF THE CREEDE FORMATION

By

James L. Conca[1]
Washington State University Tri-Cities
Richland, WA

[1]Present address:
Los Alamos National Laboratory
115 N. Main street, Carlsbad, NM 88220

ABSTRACT

Direct measurements were made of the hydraulic conductivity of Creede Formation rocks using a new experimental method. The UFA™ method employs open-flow centrifugation. Centrifugation, like gravity, has the effect on a material of a whole-body force exerting equal force at all points within the sample. The equivalent gravitational force exerted throughout the sample can be chosen to be from one to four orders of magnitude higher than earth gravity (from 10 to 10,000 g). The result is an increase in rate of fluid flow equally at all points throughout the sample so that hydraulic steady state is obtained in most geologic materials in hours, even in relatively impermeable rocks or under highly unsaturated conditions. This short time allows direct measurement of transport parameters, including hydraulic conductivity, diffusion coefficient, and retardation factors, in many types of samples under most field conditions. Traditional techniques and estimation methods require months to years to obtain these data, and cannot provide data for samples at low water contents. Hydraulic conductivities in the Creede Formation rocks ranged from 10^{-12} cm/s to 10^{-7} cm/s (10^{-9} Darcy to 10^{-4} Darcy) and showed no correlation with any other physical or mineralogical properties including porosity. The high degree of alteration to clay minerals appears to obscure any porosity/permeability relationship of the kind that occurs in many petroleum reservoir rocks. However, down-hole neutron porosities correlated well with laboratory-determined porosities and indicates the reliability of down-hole neutron methods.

INTRODUCTION

The objective of this investigation was to determine the hydrologic transport parameters of Creede formation rocks for use in transport model development and for image analysis of transport pathways to produce a porosity/permeability evolution curve in support of geochemical and isotopic water/rock interaction models. This project directly measured the hydraulic conductivity, the diffusion coefficient and the actual fluid flow paths in rocks of the Creede Formation using recently developed open-flow centrifugation techniques (the UFA™, ASTM D6527-1). Samples were investigated from the two deep drill holes into altered and unaltered Creede formation rocks from each of the units of interest, i.e., tuffs, volcaniclastics, megabreccias and other collapse-derived units.

METHODOLOGY

Transport parameters have traditionally been difficult to measure in fractured and porous media, and have generally been inferred from porosity information. The UFA, based on open-flow centrifugation, can directly determine hydraulic conductivity. The UFA achieves hydraulic steady state in a few hours for most geologic materials, even those with very low water or fluid contents (Conca and Wright 1992; Nimmo et al. 1987). There are specific advantages to using an acceleration as a fluid driving force. It is a body force similar to gravity and, so, acts simultaneously over the entire system and independently of other driving forces, e.g., gravity or matric potential. Although the centrifugal force is usually thought of as an inertial effect in the non-rotating frame, it is a real force in the rotating frame of reference of the sample. Centrifugation has been used to investigate potential relationships in soils and rocks for over 60 years (Russell and Richards, 1938). However, the use of centrifugation to measure steady state hydraulic conductivity on various porous media has only recently been demonstrated, for soils by Nimmo and co-workers (Nimmo et al., 1987) and for sediments and rocks by Conca and co-workers (Conca and Wright, 1992).

The UFA instrument consists of an ultracentrifuge with a constant, ultralow flow pump that provides fluid to the sample surface through a rotating seal assembly and microdispersal system (Figure 1). The ultracentrifuge can reach accelerations of up to 20,000 g (soils are generally run only up to 1,000 g, an effective hydrostatic pressure of only 2.5 bars), temperatures can be adjusted from -20° to 150°C, and constant flow rates can be reduced to 0.001 ml/h. Effluent from the sample is collected in a transparent, volumetrically-calibrated chamber at the bottom of the sample assembly. Using a strobe light, an observer can view the chamber while the sample is being centrifuged. Materials can be run in the UFA as recomposited samples or as samples that have been subcored directly into the sample UFA chamber. Whole rock cores and cores of ceramics, grouts, and other solids are cast in an appropriate epoxy sleeve for use in the UFA. The UFA Method is effective because it allows the operator to control the variables of flux and driving force in Darcy's Law. Darcy's Law states that the fluid flux equals the hydraulic conductivity times the fluid driving force.

Under an acceleration in which water is driven by both the matric potential gradient and the centrifugal force per unit volume, $\rho\omega^2 r$, Darcy's Law is

$$q = -K(\psi)\,[d\psi/dr - \rho\omega^2 r]$$

where q is the flux density into the sample, K is the hydraulic conductivity, ψ is the matric potential, $d\psi/dr$ is the matric potential gradient, $\rho\omega^2 r$ is the centrifugal force per unit volume, r is the radius from the axis of rotation, ρ is the fluid density, and ω is the rotation speed in radians per second. Hydraulic conductivity can be presented as a function of either the matric potential or the volumetric water content. If sufficient flux density exists, the matric potential is much less than the acceleration, $d\psi/dr << \rho\omega^2 r$. Therefore, Darcy's Law may be approximated by $q = -K(\psi)\,[-\rho\omega^2 r]$ under these conditions. Rearranging the equation and expressing hydraulic conductivity as a function of volumetric water content, θ, Darcy's Law becomes

$$K(\theta) = q/\rho\omega^2 r$$

As an example, a homogeneous silt accelerated to 2500 rpm with a flow rate of 0.01 ml/h achieved hydraulic steady state in 10 hours at a target volumetric water content of 16.4% and an unsaturated hydraulic conductivity of 4×10^{-10} cm/s. The water content distribution in the sample was homogeneous to within ±1%. Appropriate values of rotation speed and flow rate into the sample can be chosen to obtain desired values of flux density, water content, and hydraulic conductivity within the sample. Previous studies have verified the linear dependence of hydraulic conductivity on flux and the second order dependence on rotation speed. This method provides hydraulic conductivity to within ±8% at a volumetric water content known to within ±2% (Nimmo and Akstin, 1988). The high accuracy comes from the tight control on flow rate (±1% non-pulsating) and rotation speed (±5 rpm) and the ability to measure weight to ±0.001 g.

$K(\theta)$ relationships that are known with any reliability have applications beyond the immediate knowledge of hydraulic conductivity. $K(\theta)$ relationships can be compared with field moisture contents to yield information on subsurface flux or infiltration. Comparisons between samples can be made to investigate transport behavior of various fluids and contaminants. $K(\theta)$ relationships can be used to investigate pore connectivity and grain packing issues or fracture versus matrix characteristics in rock or concrete.

The UFA is a flux-controlled system and is open at either end. The pressures at the top and bottom of the sample are not fixed at any particular value. The matric potential at all points throughout the sample is allowed to attain whatever magnitude is in equilibrium with the choice of flux and rotation speed. Because the driving force is an acceleration, the bottom of the sample does not need to saturate in order for water to leave the sample, or the saturated layer is ultrathin, removing the effect in traditional soil columns that $\psi = 0$ for a significant amount of sample at the bottom of the sample. Although the acceleration can be used to calculate an equivalent pressure for comparison with the matric potential, the acceleration is not a pressure, but is a body force acting at all points simultaneously within the system, whereas the matric potential is a surface force acting as a function of distance and is slow to respond to changes in pressure or in water content especially at low water contents. In the UFA, redistribution of water and attainment of hydraulic steady-state occurs rapidly, within hours, in response to the imposed acceleration and flux. The water content within the sample also attains the steady-state value at every point, and $d\psi/dr \rightarrow 0$ throughout the sample. If the sample is homogeneous, then the water content will be uniform throughout the sample and is easily measured (Nimmo et al., 1987; Conca and Wright, 1992). In the hundreds of relatively homogeneous samples measured thus far at all speeds and fluxes, water content has been uniform to within ±1%. This indicates that the system is very close to $d\psi/dr = 0$ and that any buildup of water at the sample bottom is negligible. If the sample is heterogeneous, such as a silt lense in a coarse sand or a fractured tuff rock core, then each component reaches its own steady-state water content, but $d\psi/dr$ still approaches zero throughout the sample.

It should be noted that the use of the UFA to achieve hydraulic steady-state with a flux is completely different than the use of centrifuges to measure the matric potential, or water retention, as is traditionally done for the petroleum industry, by not having flow into the sample while it is spinning. Without a flux into the sample, there is no steady-state and there will be a non-uniform water distribution from top to bottom.

COMPARISON OF UFA METHOD WITH TRADITIONAL TECHNIQUES

Comparisons between centrifuge methods, column methods, van Genuchten/Mualem estimations and lysimeter measurements on the same materials, both soils and rocks, have shown very good agreement (Nimmo *et al.* 1994; Wright *et al.* 1994; Lindenmeier *et al.* 1995; Khaleel *et al.* 1995; Conca and Wright 1998). Most water retention data was obtained using traditional methods, e.g., Tempe cells, pressure plates, hanging water columns, and psychrometry. As an example, Figure 2 shows some results for three rock core splits from the same split-spoon core sample of non-welded Bandelier volcanic tuff. The three rock samples were run using the UFA on a whole rock core (G5-32-1), the UFA on a whole rock core pulverized and recompacted to the same density (G5-32-1), and a whole rock core run with a van Genuchten/Mualem estimation using water retention data (G5-32-3, courtesy of Daniel B. Stephens and Associates). It is noteworthy that all agree well for a material that is not a soil, given that these estimation techniques were developed for loamy soils. Also, the recompacted core behaved almost identically to the whole rock cores, supporting the notion that, being a non-welded friable tuff, from the perspective of a predictive model this rock might be considered little more than a cemented soil. This has significance to the Creede samples insofar as many were also friable volcanics. The only significant difference among these three core samplers from Figure 2 is between the saturated water contents determined during the measurement of the saturated hydraulic conductivities, which were determined separately using constant head methods (Klute and Dirksen 1986) but also agree very well for these types of measurements.

RESULTS

Twenty plugged cores, seventeen from CCM-1 and three from CCM-2, have been run in the UFA to determine hydraulic conductivity. The data are given in Table 1. Figure 3 shows the porosity as a function of the permeability (given as the hydraulic conductivity, K). There is no discernable relationship between porosity and permeability in these samples. This has been observed in other materials where significant clay minerals occur (Conca and Wright, 1992). The six samples from 1129.6' to 1150.8' correspond to a peculiar anomaly in the resistivity log over that depth range which goes through a continuous and almost constant increase. Therefore, the permeability was plotted against resistivity for all samples and is shown in Figure 4. Again, there is no correlation. Figures 5 and 6 show the permeability plotted against magnetic susceptibility and depth, illustrating that no correlations exists. Geophysical data was provided by Dr. Philip Nelson of the United States Geological Survey.

The hydraulic conductivity results show that clay alteration products dominate the present permeability characteristics of the Creede Formation, making the samples less permeable than anticipated. The 1304.9' and the 1306.9' samples are two petrologically similar samples on either side of a major alteration zone that visually left the 1306.9' sample pink and obviously altered. While the alteration dramatically increased the porosity from less than 20% to over 40%, the permeability increased by only a factor of four, a very small difference. Even more problematic are two samples, at 1141.5' and 1144.5', that have extremely different permeabilities, 4.8×10^{-12} cm/s and 3.9×10^{-8} cm/s, respectively, but are identical in every other way: mineralogically, physically, color, density, porosity, alteration mineralogy, in hand specimen and in thin section. The only difference observed between the two specimens was under the scanning electron microscope, where dissolved glass shards in the sample from 1144.5' formed slightly larger pores, the authigenic minerals were more euhedral and the smectite minerals had not grown across the pore spaces as much as in the sample from 1141.5' (Figures 7 and 8; Dr. Laura Crossey performed the SEM work at the University of New Mexico.). This is a seemingly minor effect that would ordinarily escape notice, but it apparently has severely effected the permeability and probably resulted from a slight difference in alteration history involving fluid migration rates and/or local aqueous chemistry. This indicates that generalizations based on bulk rock properties will often be misleading.

The most important result of this study is the observation that the borehole neutron porosity determinations matched the laboratory-determined saturated porosity measurements very well (Figure 9). Differences may result from the inclusion of structural water in the neutron measurement that does not reflect actual porosity and/or incomplete drying, or the loss of structural water during drying, in the laboratory, or the fact that the borehole neutron porosity measures and averages a much larger volume than individual cores in the laboratory. But generally, borehole neutron porosity is a good measure of rock porosity.

CONCLUSIONS

Hydraulic conductivities in cores from the Creede Formation investigated in this study ranged from 10^{-12} cm/s to 10^{-7} cm/s. These results for twenty cores run on the Creede Formation rocks from the Creede moat drill holes illustrate that there is no correlation between permeability and any other physical or mineralogical property including porosity, petrology, alteration mineralogy, resistivity, magnetic susceptibility, density or depth. The permeability is a function of each samples unique geologic and alteration history and broad generalizations concerning permeability will be non-defensible.

Acknowledgements - I would like to thank Laura Crossey and Phil Nelson for providing data and insightful discussions. This work was funded by the Geosciences Research Program through the Office of Basic Energy Sciences of the United States Department of Energy.

REFERENCES

Conca, J. L., and Wright, J. V., 1992, Diffusion and Flow in Gravel, Soil, and Whole Rock: Applied Hydrogeology, Volume 1, p. 5-24.

Conca, J. L., and Wright, J. V. 1998, The UFA Method for Rapid, Direct Measurements of Unsaturated Soil Transport Properties: Australian J. of Soil Research, Volume 36, p. 291-315.

Klute, A., and Dirksen, C., 1986, Hydraulic Conductivity and Diffusivity: Laboratory Methods, *in* Methods of Soil Analysis, Part 1, Physical and Mineralogical Methods, Second Edition, ed. A. Klute, pp. 687-734, American Society of Agronomy, Inc., and Soil Science Society of America, Inc., Madison, Wisconsin.

Lindenmeier, C. W., Serne, R. J., Conca, J. L., Owen, A. T., and M. I. Wood, M. I., 1995, Solid Waste Leach Characteristic and Contaminant-Sediment Interactions, Volume 2: Contaminant Transport Under Unsaturated Conditions: Technical Report PNL-10722, Pacific Northwest Laboratory, Richland, WA.

Nimmo, J. R., and Akstin, K. C., 1988, Hydraulic conductivity of a sandy soil at low water content after compaction by various methods: Soil Science Society of America Journal, Volume 52.

Nimmo, J. R., Rubin, J., and Hammermeister, D. P., 1987, Unsaturated Flow in a Centrifugal Field: Measurement of Hydraulic Conductivity and Testing of Darcy's Law: Water Resources Research, Volume 23, p. 124-134.

Nimmo, J. R., Stonestrom, D. A., and Akstin, K. C., 1994, The Feasibility of Recharge Rate Determination Using the Steady-State Centrifuge Method: Soil Science Society of America Journal, Volume 58, p. 49-56.

RUssell, M. B., and Richards, L. A., 1938, The Determination of Soil Moisture Energy Relations by Centrifugation: Soil Science Society of America Proceedings, Volume 3, p. 65-69.

Van Genuchten, M. Th., Leij, F.J., and Lund, L.J., 1992, .Indirect Methods for Estimating the Hydraulic Properties of Unsaturated Soils: Proceedings of the International Workshop on Indirect Methods for Estimating the Hydraulic Properties of Unsaturated Soils, University of California, Riverside.

Wright, J. V., Conca, J. L. and Chen, X., 1994, Hydrostratigraphy and Recharge Distributions from Direct Measurements of Hydraulic Conductivity Using the UFA™ Method, PNL Technical Report PNL-9424, Pacific Northwest Laboratory, Richland, WA (1994).

FIGURE CAPTIONS

Figure 1. The UFA™ rotor and seal assembly.

Figure 2. Hydraulic conductivity results using the UFA and van Genuchten/Mualem methods on splits of the same rock core.

Figure 3. Neutron porosity versus permeability, given as hydraulic conductivity, for samples of the Creede Formation, showing no apparent relationship. Designation and depth are shown for each sample. (cm/s = 1033 Darcy)

Figure 4. Resistivity versus permeability, given as hydraulic conductivity, for samples of the Creede Formation, showing no apparent relationship.

Figure 5. Magnetic susceptibility versus permeability, given as hydraulic conductivity, for samples of the Creede Formation, showing no apparent relationship.

Figure 6. Depth versus permeability, given as hydraulic conductivity, for samples of the Creede Formation, showing no apparent relationship.

Figure 7. Scanning electron micrograph of the sample at 1144.5 ft. from the Fallout A unit showing porosity formed from dissolution followed by authigenic mineral formation. Electron micrograph by Laura Crossey.

Figure 8. Scanning electron micrograph of the sample at 1141.5 ft. from the Fallout A unit showing porosity formed from dissolution followed by authigenic mineral formation. Note the difference in morphology compared to the previous figure and the pore-spanning authigenic minerals. Both samples are identical in hand specimen, density, porosity, color and mineralogy, but differ in their permeabilities by about four orders of magnitude. Electron micrograph by Laura Crossey.

Figure 9. Neutron porosity versus porosity determined in the laboratory by saturating with groundwater for two months. The agreement is very good considering the amount of structural water contained in the minerals of these altered volcanics which can contribute to errors in both methods.

TABLE 1

Creede Sample	Depth (ft)	K (cm/s)	Lab Poros. (%)	Neutron Poros. (%)	Mag. Susc. (SI units)	Resistivity (ohm-m)
1R66-A4.15	-585.65	1.12e-7	33.3	34.9	14.369	35.366
1R127-A8.05	-1129.6	1.13e-8	29.1	31.4	15.016	6.104
1R128-A4.2	-1134.7	8.04e-12	29.2	33.3	563.07	5.528
1R129-A1.0	-1141.5	4.82e-12	20.4	25.1	944.82	16.213
1R129-A4.0	-1144.5	3.86e-8	23.6	23.3	982.73	22.803
1R129-A7.6	-1148.1	9.36e-9	14.5	23.2	351.14	28.597
1R130-A0.3	-1150.8	2.25e-10	26.8	31.8	224.25	11.698
1R145-A4.4	-1304.9	1.28e-8	22.3	17.3	1247.4	97.097
1R145-A6.4	-1306.9	5.37e-8	43.4	44.6	348.82	29.312
2R159-A1.5	-1601.5	1.23e-8	35.8	37.1	82.214	8.133
2R102-5.1v	-1056.6	1.23e-9	21.7			
2R102-5.2h	-1056.7	3.13e-9	26.6			
1R131-A0.55	-1159.1	5.9e-10	30.4	34.0	88.858	4.053
1R131-A10.3	-1168.8	4.79e-10	27.2	31.0	587.81	5.932
1R132-A9.6	-1178.1	7.04e-10		31.7	966.88	10.419
1R134-A5.3	-1193.8	4.87e-10	23.7	32.8	1374.5	9.431
1R135-A3.8	-1202.8	1.23e-9	22.8	31.9	1475.7	18.438
1R135-A6.7	-1205.7	3.43e-10	6.8	9.5	461.84	77.057
1R136-A4.7	-1214.2	1.48e-9		5.4	562.39	282.75
1R137-A4.55	-1224.1	1.37e-9	10.2	10.8	466.15	283.99

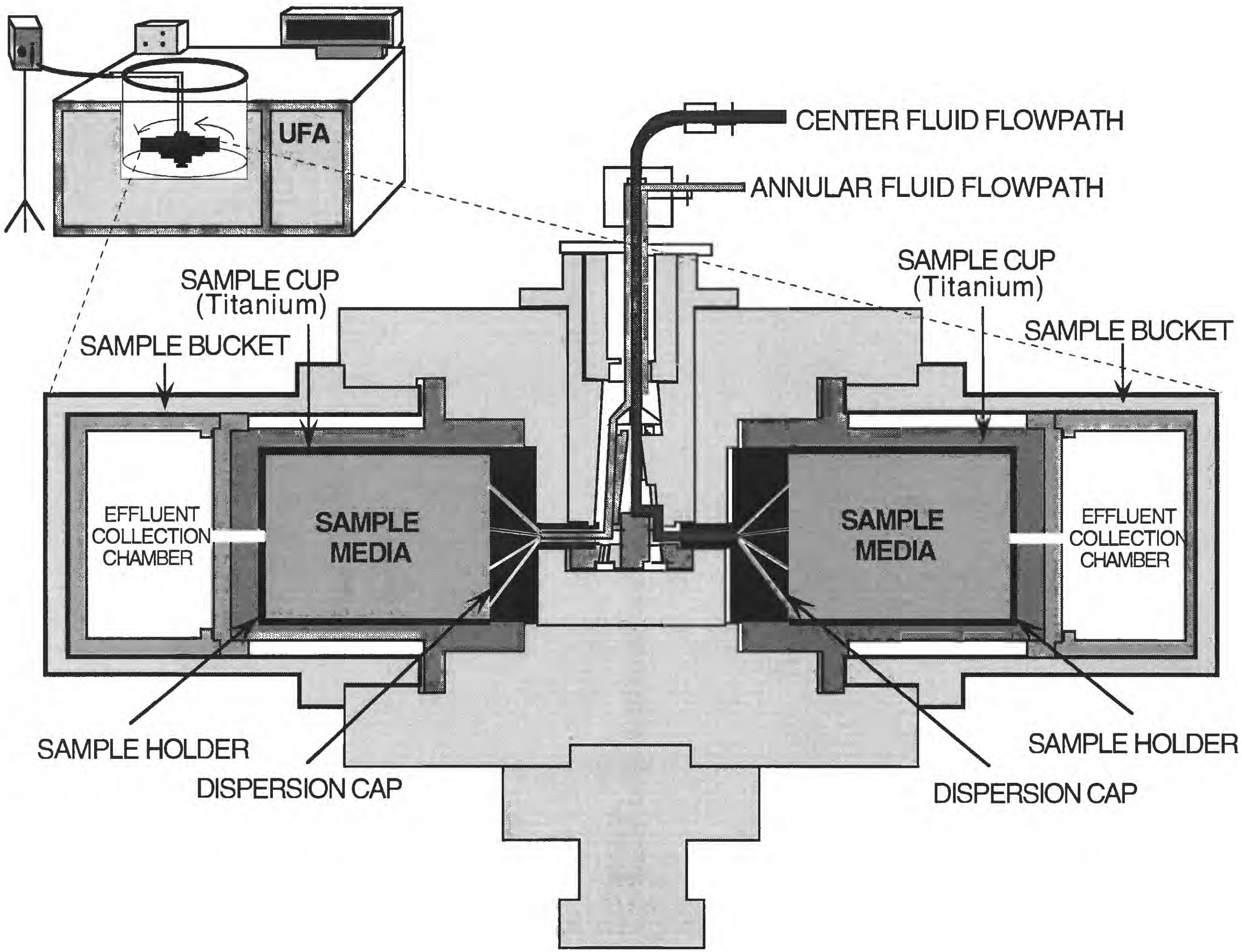
UFA
CENTER FLUID FLOWPATH
ANNULAR FLUID FLOWPATH
SAMPLE CUP
(Titanium)
SAMPLE BUCKET
SAMPLE CUP
(Titanium)
SAMPLE BUCKET
EFFLUENT
COLLECTION
CHAMBER
SAMPLE
MEDIA
SAMPLE
MEDIA
EFFLUENT
COLLECTION
CHAMBER
SAMPLE HOLDER
DISPERSION CAP
SAMPLE HOLDER
DISPERSION CAP

Figure 1

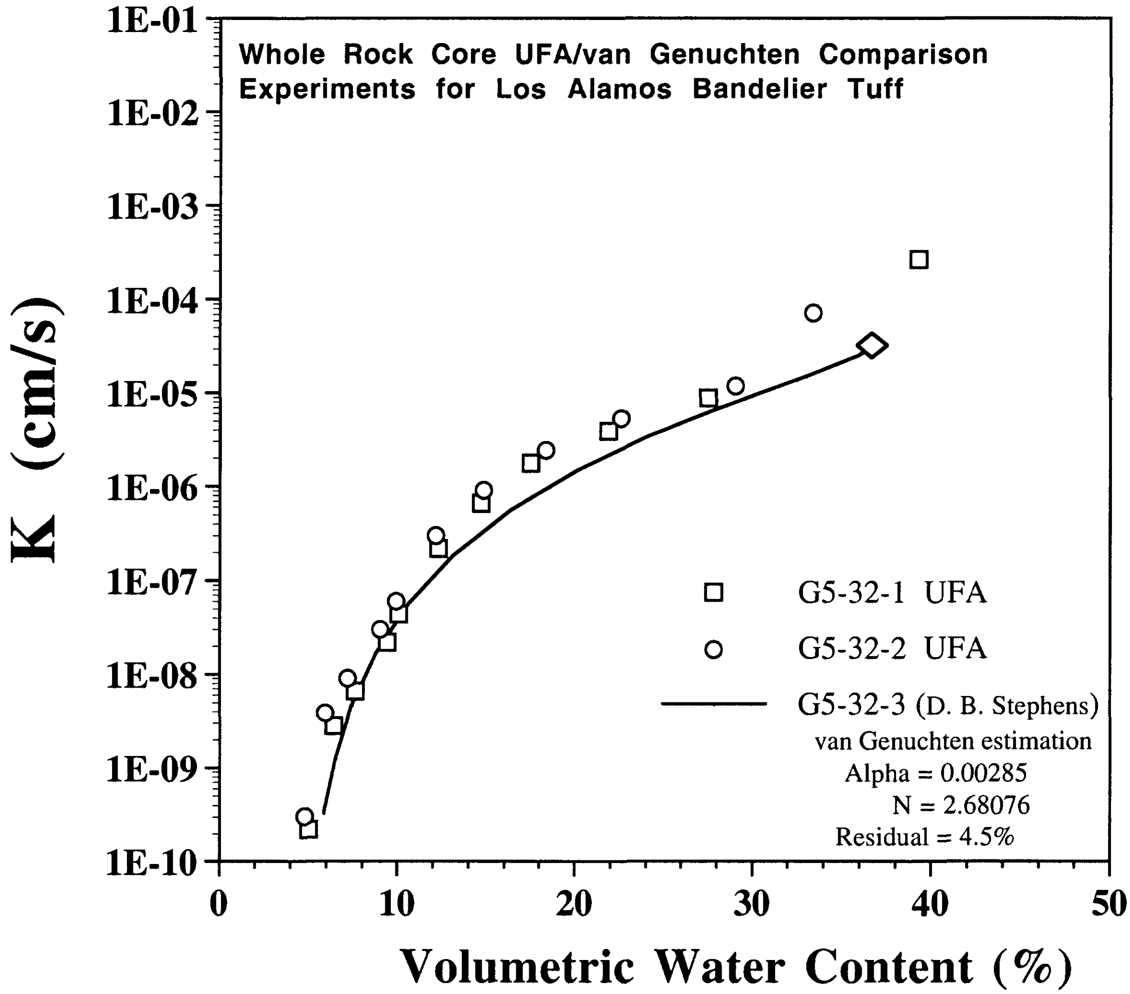

Whole Rock Core UFA/van Genuchten Comparison
Experiments for Los Alamos Bandelier Tuff
K (cm/s)
1E-01
1E-02
1E-03
1E-04
1E-05
1E-06
1E-07
1E-08
1E-09
1E-10
0
10
20
30
40
50
Volumetric Water Content (%)
G5-32-1 UFA
G5-32-2 UFA
G5-32-3 (D. B. Stephens)
van Genuchten estimation
Alpha = 0.00285
N = 2.68076
Residual = 4.5%

Figure 2

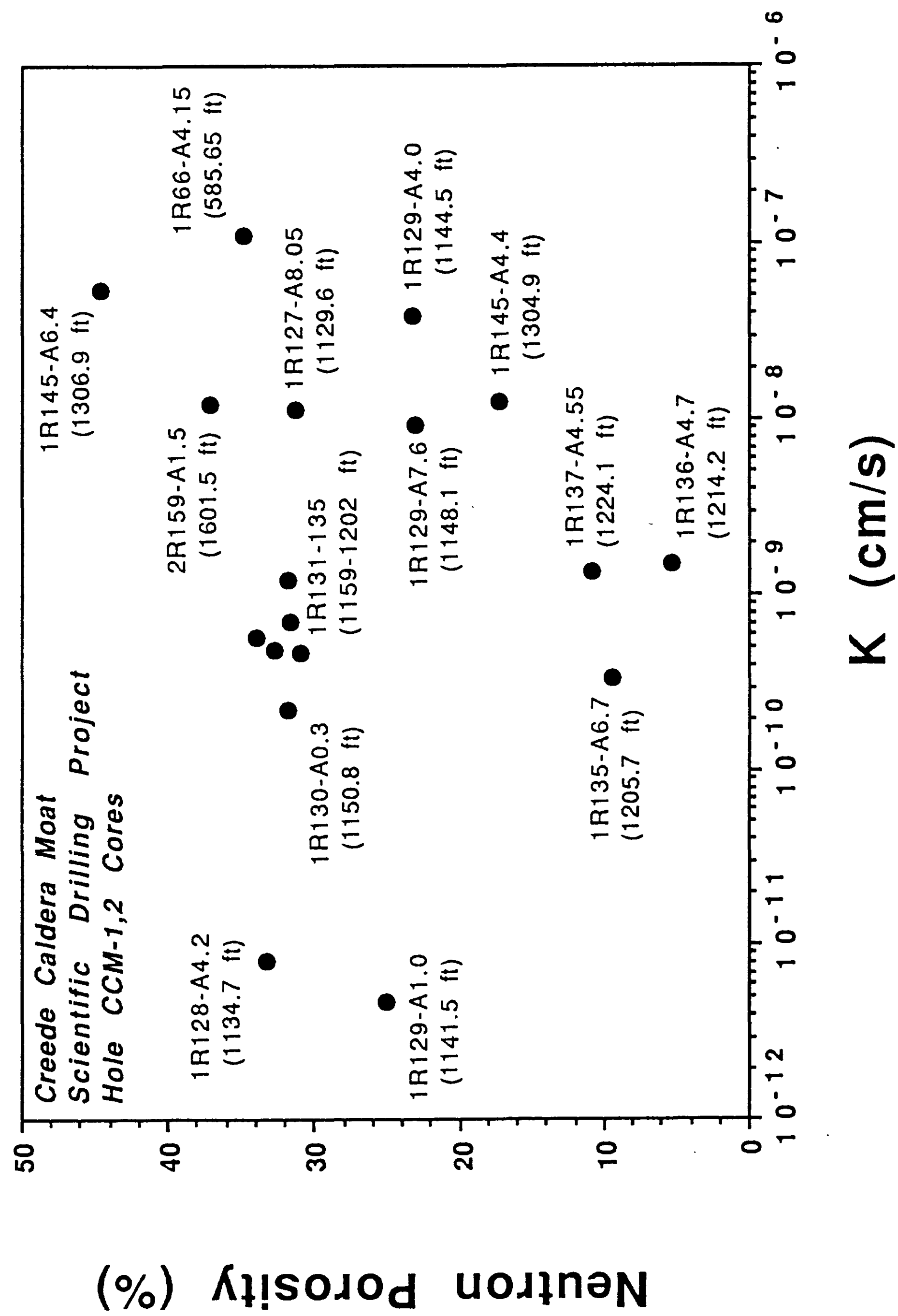
Creede Caldera Moat
Scientific Drilling Project
Hole CCM-1,2 Cores
1R128-A4.2 (1134.7 ft)
1R129-A1.0 (1141.5 ft)
1R130-A0.3 (1150.8 ft)
1R135-A6.7 (1205.7 ft)
1R131-135 (1159-1202 ft)
2R159-A1.5 (1601.5 ft)
1R129-A7.6 (1148.1 ft)
1R137-A4.55 (1224.1 ft)
1R136-A4.7 (1214.2 ft)
1R145-A6.4 (1306.9 ft)
1R127-A8.05 (1129.6 ft)
1R145-A4.4 (1304.9 ft)
1R66-A4.15 (585.65 ft)
1R129-A4.0 (1144.5 ft)
Neutron Porosity (%)
K (cm/s)
50
40
30
20
10
0
10-12
10-11
10-10
10-9
10-8
10-7
10-6

Figure 3

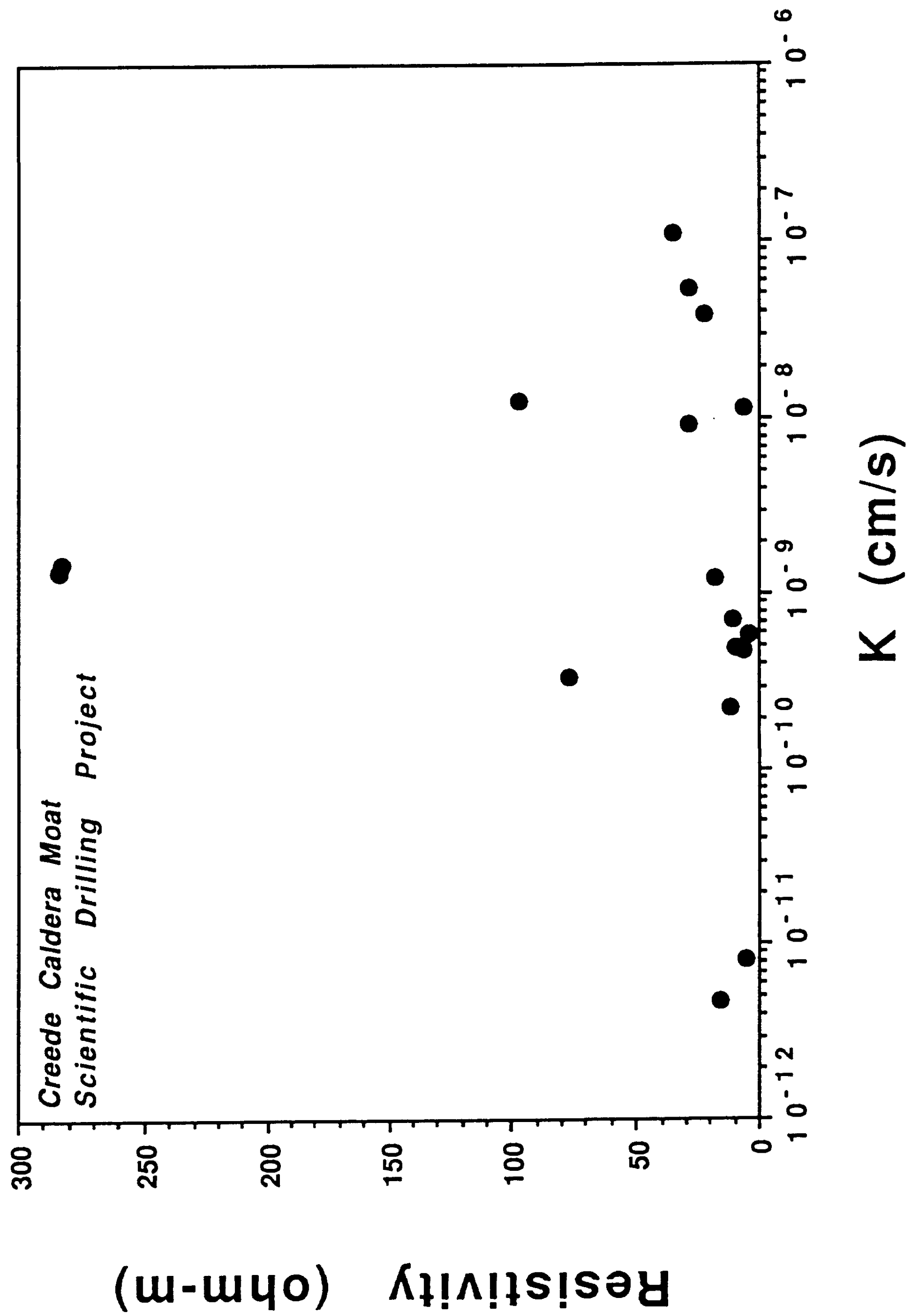

Creede Caldera Moat
Scientific Drilling Project
Resistivity (ohm-m)
300
250
200
150
100
50
0
K (cm/s)
10-12
10-11
10-10
10-9
10-8
10-7
10-6

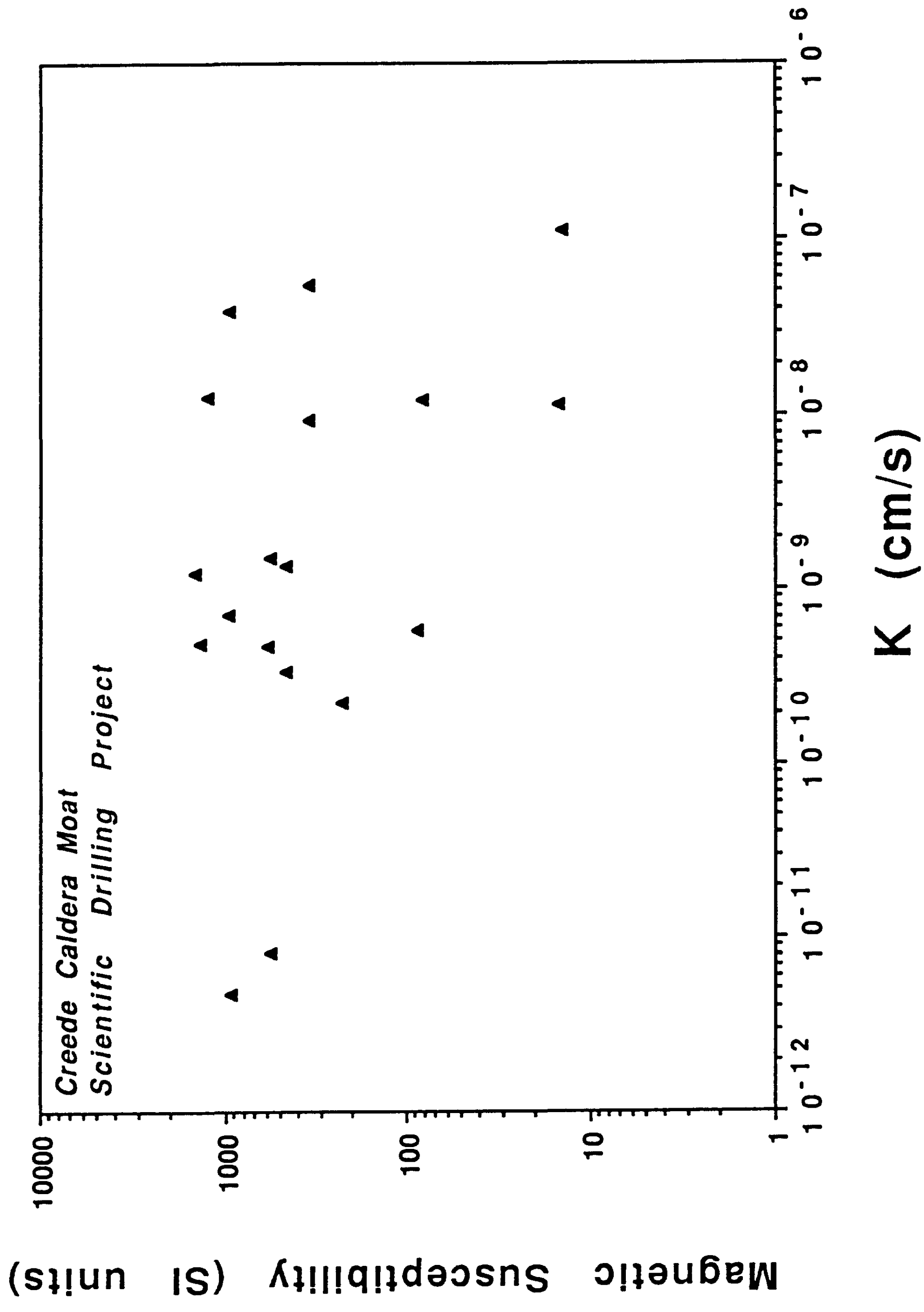
Creede Caldera Moat
Scientific Drilling Project
Magnetic Susceptibility (SI units)
10000
1000
100
10
1
K (cm/s)
10-12
10-11
10-10
10-9
10-8
10-7
10-6

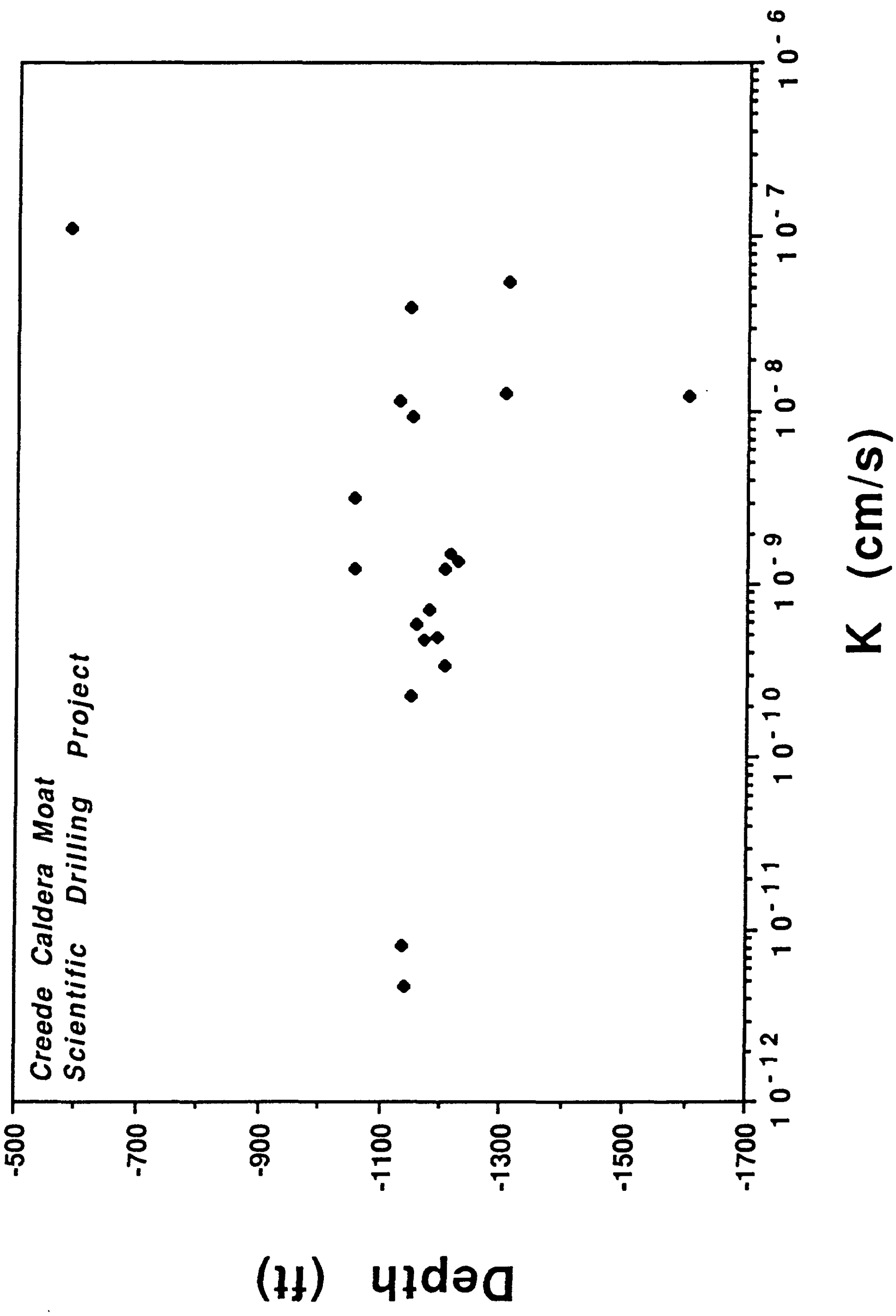
Creede Caldera Moat
Scientific Drilling Project
Depth (ft)
-500
-700
-900
-1100
-1300
-1500
-1700
K (cm/s)
10⁻¹²
10⁻¹¹
10⁻¹⁰
10⁻⁹
10⁻⁸
10⁻⁷
10⁻⁶

CCM-1 1144.5 ft K=1.2x10^{-8} cm/s

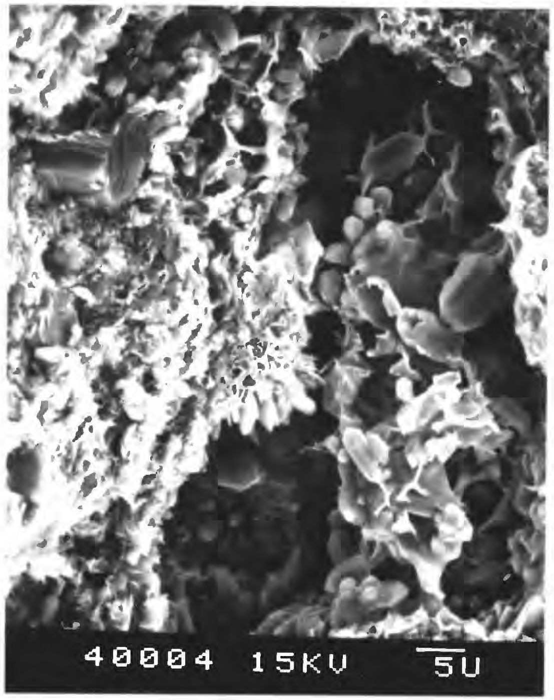

Figure 7

CCM-1 1141.5 ft K=1.5x10^{-12} cm/s

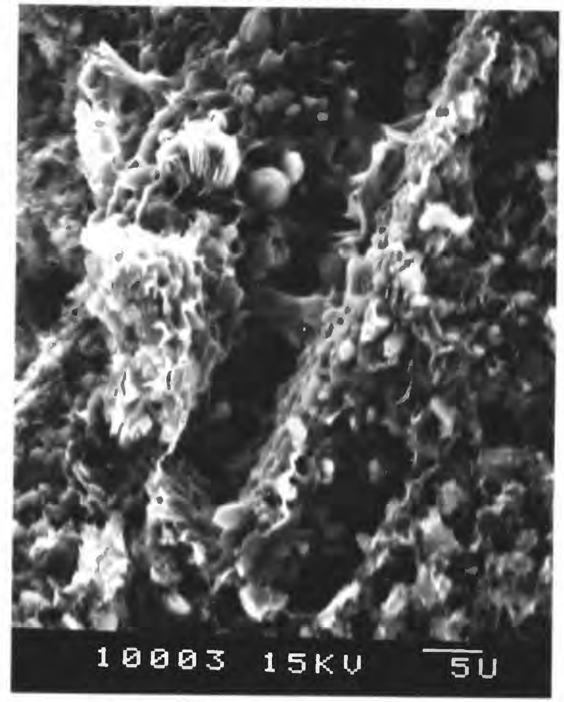

Figure 8

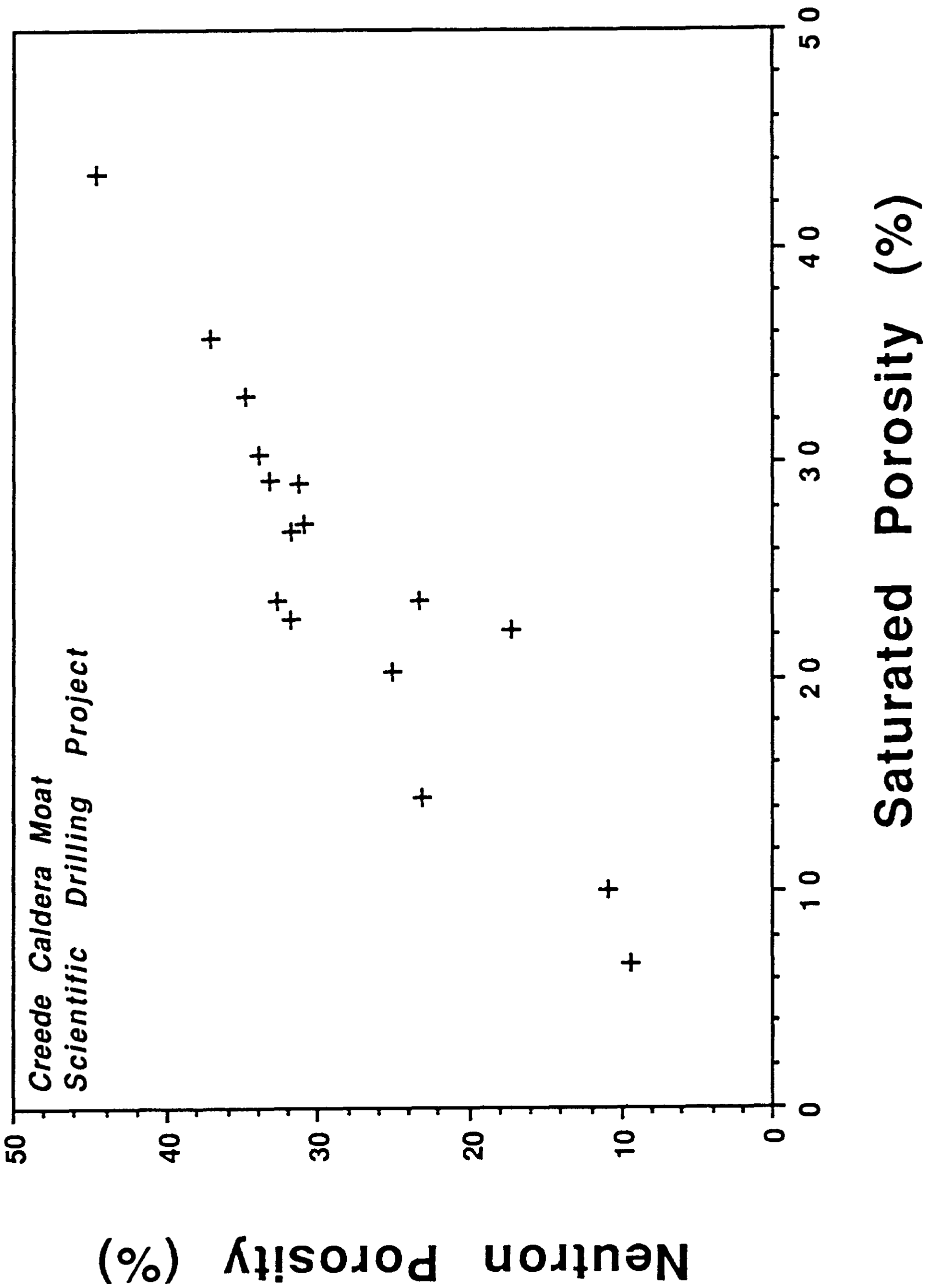
Creede Caldera Moat
Scientific Drilling Project
Neutron Porosity (%)
Saturated Porosity (%)
0
10
20
30
40
50